Statistical Spectral Fitting of Brown Dwarf Binary Candidates

John-Michael Eberhard

A senior thesis submitted to the faculty of
Brigham Young University
in partial fulfillment of the requirements for the degree of

Bachelor of Science

Denise Stephens, Advisor

Department of Physics and Astronomy

Brigham Young University

ABSTRACT

Statistical Spectral Fitting of Brown Dwarf Binary Candidates

John-Michael Eberhard
Department of Physics and Astronomy, BYU
Bachelor of Science

Brown dwarf binary systems provide key insights into the formation and evolution of brown dwarfs. To discover more binary systems, brown dwarf atmospheric models were fitted to the observed spectra of several brown dwarf systems. Spectral data for the systems was retrieved from the SpeX Spectral Library, the InfraRed Telescope Facility Library and the InfraRed Spectral Archive. The collected models predicted the spectrum a singular brown dwarf would have based on its temperature, surface gravity, cloud density, and amount of convection in the atmosphere. Binary models were created from the singular models and all of the models were compared to the observed spectra. Using a chi-squared analysis, the goodness of fit was calculated for each model. The best binary and singular fits were compared, and statistical analysis was performed to determine at what level of confidence each system could be claimed as binary. Twenty-six systems were studied and seven were found to be binary at a 99% confidence level: 2MASS 05591914-1404488, SDSS J042348.57-041403.5, 2MASSW J0320284-044636, 2MASS 14313097+1436539, DENIS-P J225210.73-173013.4, 2MASS 20282035+0052265, and SDSS J141624.08+134826.7. The method proved to be effective and can be used to more efficiently discover brown dwarf systems.

Keywords: 2MASS 05591914-1404488, SDSS J042348.57-041403.5, 2MASSW J0320284-044636, 2MASS 14313097+1436539, DENIS-P J225210.73-173013.4, 2MASS 20282035+0052265,SDSS J141624.08+134826.7, brown dwarf binary, spectral fitting

ACKNOWLEDGMENTS

I thank my advisor Dr. Denise Stephens for her support and her husband Tom Stephens for helping understand the computer code.

Contents

Table of Contents **iv**

List of Figures **v**

List of Tables **v**

1 Introduction **1**
- 1.1 Brown Dwarfs . . . 1
- 1.2 Spectroscopic and Photometric Analysis . . . 3
- 1.3 Previous Work at BYU . . . 4
- 1.4 Overview . . . 5

2 Data Retrieval and Analysis **7**
- 2.1 Spectral Telescopes . . . 7
- 2.2 Spectral Conversion . . . 9
- 2.3 Brown Dwarf Atmosphere Models and Parameters . . . 11
- 2.4 Adjusting the Atmospheric Models . . . 14
- 2.5 Fitting Models to the Data . . . 18
- 2.6 Statistical Analysis . . . 21

3 Results and Future Work **24**
- 3.1 Identified Binary Systems . . . 24
- 3.2 Comparison to Previous Results . . . 26
- 3.3 Future Work . . . 27

Bibliography **31**

Index **33**

List of Figures

1.1 Brown Dwarf Cooling Curves 2

2.1 A Basic Spectrograph 8

2.2 Convolution of Spectral Data and Filter Profiles 12

2.3 Creation of Binary Models 15

2.4 Smoothing Atmospheric Models 16

2.5 Spectrum for SDSSp J042348.57-041403.5 17

2.6 Comparison of Binary and Singular Fits for 2MASS 14313097+1436539 20

2.7 Comparison of Binary and Singular Fits for 2MASS 05591914-1404488 21

2.8 Probability Distribution for η_{sb} 23

List of Tables

3.1 Confidence Levels for Discovered Binary Systems 28
3.2 Best Fit Binary Models for Discovered Binary Systems 29
3.3 Best Fit Singular Models and Optical Spectral Types for Discovered Binary Systems 29
3.4 Comparison of Confidence Levels for Binary Systems 30

Chapter 1

Introduction

1.1 Brown Dwarfs

Brown dwarfs are celestial bodies with masses and temperatures between that of stars and planets. With masses 13 to 80 times the mass of Jupiter, they are far less massive than the smallest stars, but they form in a manner completely different from any planet. Like a star, a brown dwarf begins to form when a giant molecular cloud collapses under its own gravity. In stellar formation, nuclear fusion begins at the center of the cloud and creates an outward pressure which pushes back against the force of gravity. The two forces balance in a state known as hydrostatic equilibrium, and a star is created. In brown dwarf formation, the mass of the collapsing cloud is not large enough to initiate hydrogen fusion, and electron degeneracy pressure pushes back against the inward pull of gravity. When the electron degeneracy pressure equals the pressure caused by gravity, the sphere of gas becomes stable and forms a brown dwarf.

Without hydrogen fusion to produce an internal source of energy, most brown dwarfs continuously cool after their formation. Some massive brown dwarfs fuse deuterium, an isotope of hydrogen, for up to a hundred million years after their formation, but after that time they cool for

the rest of their lifetimes. Brown dwarfs in this sense are more similar to planets than to stars, as planets also cool after formation because they do not fuse hydrogen. Figure 1.1 shows the way that the temperatures of brown dwarfs decrease over time; it was taken from Philips *et al.* (2020).

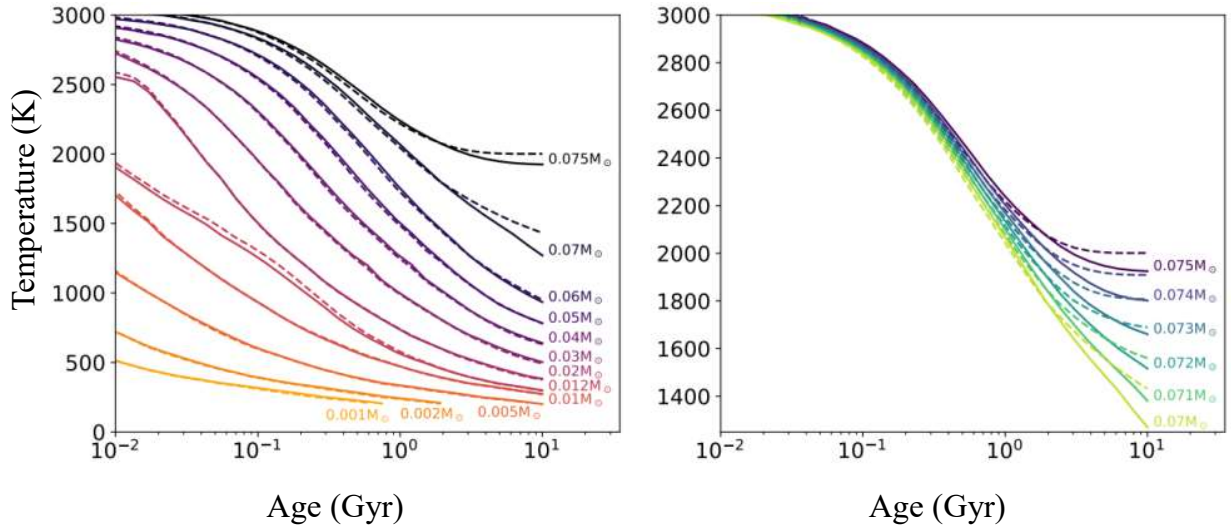

Figure 1.1 Plots of temperature versus age for brown dwarfs with different masses. Since brown dwarfs cannot fuse hydrogen, their temperatures decrease after the brown dwarfs form. Larger brown dwarfs fuse deuterium for a time and retain higher temperatures, but once the fusion is completed, they cool like the smaller dwarfs.

Because their temperatures and luminosities are less than that of stars, brown dwarfs are difficult to detect and study. Consequently, they remained only a theoretical concept until the first one was discovered in 1995. (Rebolo et al. 1995)

Since then, research regarding brown dwarfs has flourished, and as more have been discovered, they have been divided into three main spectral types. Stars are divided into different spectral types based on their effective temperatures, where effective temperature is defined as the temperature that a pure blackbody would need to have to emit the same amount of electromagnetic radiation as the object being observed. From hottest to coldest, the spectral types of stars are O, B, A, F, G, K, and M. Brown dwarfs add on to the end of the sequence and include the L (2400-1400 K), T (1400-500 K), and Y (500-125 K) spectral types. Subdivisions of spectral types are specified by including a

digit between 0 and 9 after the letter, where 0 represents the hottest objects and 9 represents the coolest.

As more brown dwarf systems are discovered, questions about them continue to arise, since many of the systems do not match current formation models. For example, from observations of stars in the nearby galaxy, astronomers have found that low mass stars greatly outnumber high mass stars and there appears to be a correlation between mass and quantity: the higher the mass of an object, the less common it is. (Thies et al. 2015) This correlation is known as the Initial Mass Function (IMF). Brown dwarfs are a notable exception to the IMF. Though brown dwarfs have smaller masses than any M star, there are far fewer brown dwarfs than there are M stars. There is also an oddity known as the "brown dwarf desert" which refers to the fact that brown dwarfs rarely form in tight orbits around main sequence stars. (Thies et al. 2015). The only time brown dwarfs are found with small separations with other objects is when one brown dwarf orbits another brown dwarf, in what is known as a brown dwarf binary. The key to understanding brown dwarf formation may lie in the formation of these brown dwarf binary systems. To better understand the way these systems form and why the current formation models are inaccurate, I worked to discover binary systems and identify their properties using spectroscopy.

1.2 Spectroscopic and Photometric Analysis

Brown dwarf spectra form when the blackbody radiation produced from the core of the brown dwarf has certain wavelengths of light absorbed by particles in its atmosphere. Different elements and molecules absorb different wavelengths of light; thus, by analyzing the spectra of brown dwarfs, the composition of their atmospheres can be determined.

The spectrum of a brown dwarf depends on a few critical parameters: its effective temperature, surface gravity, amount of cloud cover, rate of convection in the atmosphere, and metallicity. The

effect each parameter has on the spectrum is discussed in more depth in Chapter 2. A single brown dwarf will have one value for each of these parameters, and will have a unique spectrum that reflects these characteristics. When the light from two brown dwarfs combine, the spectrum becomes a mix of two different values for each physical parameter. Therefore, the spectrum produced by a binary system is different that any that could be made from a single object.

There are over 2500 known brown dwarfs and I did not have time to study all of them. Instead, I established some criteria to determine which were most likely to be binary systems. To identify probable binary systems, other members of my research group searched for brown dwarfs that were overluminous, which meant they were brighter than they should have been. Overluminous brown dwarfs were good binary candidates because if a brown dwarf system was brighter than it was expected to be, it could have been brighter because the light from two brown dwarfs was combining together to make a system look like one overly bright brown dwarf.

To find overluminous candidates, members of my research group compared the luminosity each brown dwarf should have based on its spectral type to its observed luminosity. Data taken from the space telescope Gaia was used to find the distances to several brown dwarfs. Once the distance was known, the luminosity given at the surface of the brown dwarf was calculated and compared to the luminosity of the object's spectral class. If the observed luminosity of a brown dwarf was greater than the luminosity predicted by the spectral class, the brown dwarf was flagged as a target of interest. By searching through luminosity data for brown dwarfs, my group was able to identify 117 overluminous candidates that I would go on to study using spectroscopy.

1.3 Previous Work at BYU

Stephens *et al.* (2009) previously performed spectral analysis on 21 brown dwarfs to test if they were binary systems. She fit spectral data to models created by Saumon and Marley (2008) and

identified the following properties of each brown dwarf: the effective temperature, surface gravity, cloud cover amount, and convection coefficient. Of the 21 brown dwarfs studied, the following four were identified as being potentially binary systems: 2MASSW J0036159+182110 (2MASS J0036+1821), SDSS J080531.83+481233.1 (SDSS J0805+4812), SDSS J105213.51+442255.7AB (SDSS J1052+4422), and 2MASS J05591914-1404488 (2MASS 0559-1404).

Esplin (2010) built on the work done by Stephens and wrote a smoothing and fitting code in MATLAB to process the data from NASA's Spitzer Space Telescope (SST). Esplin performed the analysis on the 2MASS 0559-1404 system and found it to be a binary system.

Farnbach (2017) used the methods employed by Stephens and Esplin to fit models to the spectra of the systems Kelu-1, 2MASS 0036+1821, SDSS 0805+4812, SDSS 1052+4422, and 2MASS 0559-1404, and 2MASSW J2224438-015852 (2MASS 2224-0158). She found the temperature, surface gravity, cloud cover, and convection amount for each of these systems and calculated the goodness of fit values for the binary and singular models.

1.4 Overview

The aim of this thesis is to improve the techniques used to identify binary brown dwarf systems. I also share the binary systems I discovered and their properties. In Chapter 2, I discuss the methods I used to perform the spectral analysis and the improvements I made to the methods employed by Stephens *et al.* (2009), Esplin (2010), and Farnbach (2017). I explain how I found 26 systems that had spectral data online, used atmospheric models to create binary models, and fit singular and binary models to the data. Afterwards, I describe the statistical analysis I performed to identify binary systems at the 99% confidence level. Chapter 3 gives the results of the analysis and lists the binary systems I found, along with their properties. In Chapter 3, I also explain how this data compares to previous results, and I describe what future work can be done with brown dwarf spectral

fitting.

Chapter 2

Data Retrieval and Analysis

2.1 Spectral Telescopes

To begin my research, I downloaded brown dwarf spectral data that was collected using various telescopes with different spectrographs. A spectrograph is an instrument used to record a spectrum from the light given off by an object. A spectrograph takes incoming light and, using mirrors and a diffraction grating, spreads the light across its different wavelengths. An example of a simple spectrograph is shown in Figure 2.1, in a schematic taken from the Australia Telescope National Facility website (www.atnf.csiro.au). Incident light coming from an object is reflected off of a collimating mirror, which creates parallel light beams. The light is then spread out into its different wavelengths using a diffraction grating. The light reflects off the camera mirror and then a detector, such as a Charge Couple Device (CCD), records the intensity of light at each wavelength. A computer can then plot the spectrum. Once a spectrum is measured, it can then be used to determine which wavelengths of light the brown dwarf's atmosphere is absorbing.

Brown dwarfs are dim and difficult to study with surface telescopes. Due to their low temperatures, their blackbody radiation peaks in the near- and mid-infrared frequency, as determined by

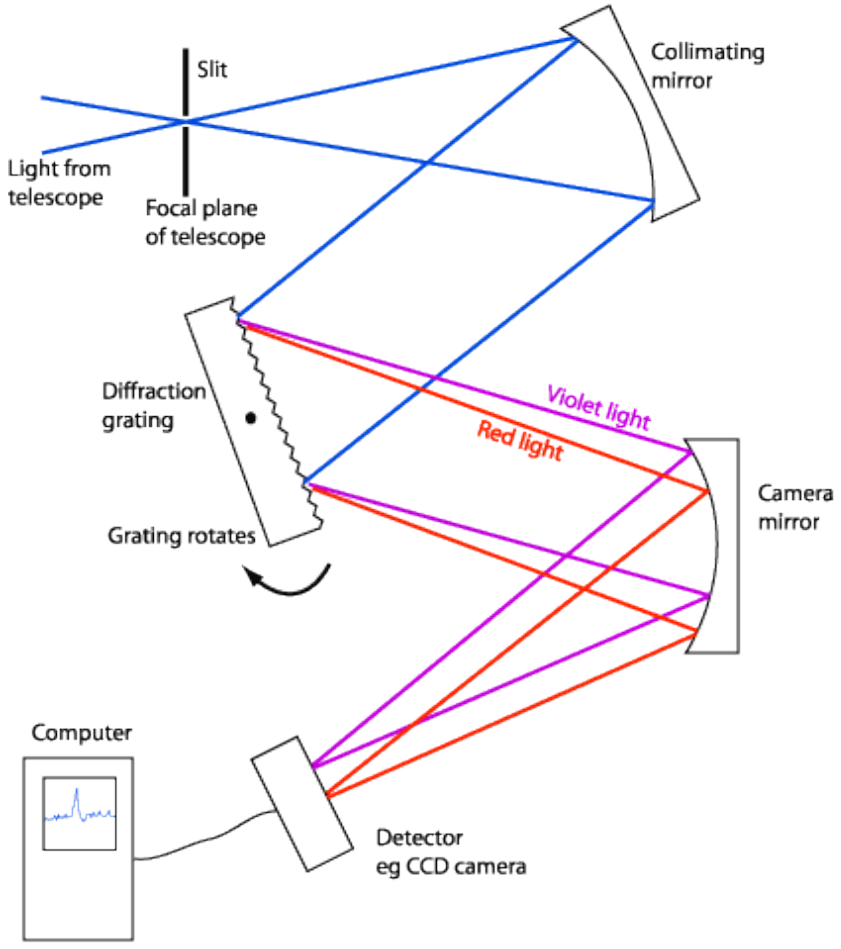

Figure 2.1 A basic spectrograph. Some spectrographs have more mirrors and filters to limit the spectrum to certain wavelengths. (www.atnf.csiro.au)

Wein's law. Wein's law states that the wavelength at which an object emits the maximum intensity of light is inversely proportional to the surface temperature of the object. Specifically, $\lambda = 0.29/T$, where λ is the peak wavelength in cm and T is the surface temperature in K. Following this calculation, brown dwarfs emit a maximum intensity of light in the infrared region of the electromagnetic spectrum. Water in the Earth's atmosphere naturally absorbs light at several infrared wavelengths and interferes with the observations, making it difficult to collect infrared spectra beyond 4 microns

with ground-based telescopes. Infrared emission from the Earth also peaks near 10 microns, and adds an additional source of noise for observations longward of 3 microns. The infrared photons emitted by molecules in Earth's atmosphere, along with the background emission from Earth, produce a large number of infrared photons that the spectrograph collects in addition to the infrared photons from the astronomical object. These additional photons create statistical noise which is not easily removed and lowers the effective signal-to-noise of our observations.

To avoid the additional sources of noise created by the Earth, space telescopes can be used to collect infrared spectra of brown dwarfs. NASA's Spitzer Space Telescope (SST) collected spectral data of brown dwarfs in the mid-infrared from 5 to 38 microns using the InfraRed Spectrograph (IRS). The majority of brown dwarfs in this study were just imaged from 5 to 14.5 microns. This data is archived in the InfraRed Science Archive (IRSA), which is publicly available.

Infrared spectral data was also collected at shorter wavelengths from ground-based telescope archives. In particular, I analyzed data collected by the SpeX spectrograph on NASA's 3-meter InfraRed Telescope Facility (IRTF). The SpeX data was chosen because the instrument is capable of acquiring a complete spectrum from 0.6-2.5 microns with just one observation of the brown dwarf. The spectral data collected by IRTF is archived in the SpeX Prism Libraries (SPL) and the IRTF Spectral Library and is publicly available.

2.2 Spectral Conversion

I collected data from IRSA (5-14.5 microns), SPL (0.6-2.5 microns), and the IRTF Spectral Library (0.6-2.5 microns) to create a composite spectrum from 0.6 to 14.5 microns for each of the brown dwarfs I studied. I also searched through several other data archives, including the Combined Atlas of Sources with Spitzer IRS Spectra (CASSIS) and the Keck Observatory Archive (KOA). The results from CASSIS directed me back to the IRSA website and provided no new data. KOA

provided pictures of the spectra as pictures in the form of Flexible Image Transport System (FITS) files, without any tables giving the numerical data. Not knowing how to obtain numerical results from FITS files, I focused on the data I extracted from IRSA, SPL, and the IRTF Spectral Library.

The data from IRSA and the IRTF Spectral Library was given in units of Janskys, but the data from SPL was normalized, which created a problem when trying to combine the short and long wavelength spectra together. A Jansky (Jy) is a unit of measurement for flux equal to 10^{-26} W m^{-2} Hz^{-1} and is used commonly in radio and infrared astronomy for small quantities of flux. The data from IRSA and the IRTF Spectral Library was given in units of Janskys, but the data from SPL was normalized, meaning the spectra had been converted into unitless spectra where the maximum flux was set to a value of 1. The fitting code I used could fit data that was either all given in proper flux units (Jy) or data that had been combined and then normalized, but it could not properly fit data that was a combination of the two because each normalized spectrum was offset by some unknown amount. To make the data usable for my code, I had to reverse the normalization process.

To accomplish this, I created a Python code, modified after one found on Astronomy Stack Exchange. In the code, I convolved the normalized fluxes with the filter data for IRTF. For telescopes, certain filters are used to restrict the light to specific ranges of wavelengths. In the infrared range, the primary filters used are known as the J (1.0-1.4 microns), H (1.5-1.8 microns), and K_s (2.0-2.3 microns) filters. For a simple idealistic filter, the filter lets 100% of the light through at the desired wavelengths and 0% everywhere else. In practice however, the ideal transmission does not occur, and filter profiles model the percentage of light that is transmitted at each wavelength. I found the filter profiles for IRTF on the IRTF website (irtfweb.ifa.hawaii.edu) and convolved the profiles with the reported spectral data to estimate the flux recorded in each of the filters after being normalized.

An example of the convolution of the normalized spectrum and the filter profiles for the brown dwarf SDSS J141624.08+134826.7 (SDSS 1416+1348) is shown in Figure 2.2. The red line shows the normalized data that was given, and the blue line shows the filter profiles for the three filters

used. The black line shows the convolution of the red and the blue lines and represents the flux that would be recorded in each filter, after the data was divided by the normalization constant. I integrated under the black line in the H and K_s filters to determine the flux that would be reported after the normalization constant was applied to the observed flux. I converted these normalized fluxes into magnitudes and compared these normalized magnitudes to the recorded magnitudes of the brown dwarfs in the H and K_s filters. I found the ratio between the actual magnitudes and the normalized magnitudes, which gave me the normalization constant that the original data had been divided by. The J filter magnitude was discarded for this calculation, since the J filter is sensitive to the amount of water vapor in the Earth's atmosphere. Small variations in water greatly affected the magnitudes and skewed the results, so that the normalization constant found for the J filter did not match the normalization constant found using the H and K_s filters. Once I determined the normalization constant, I multiplied the original normalized data by the constant to obtain the spectral data in units of Janksys.

2.3 Brown Dwarf Atmosphere Models and Parameters

With the spectral data collected and converted to the proper units, I next had to find models to compare against the spectral data. As was done by Esplin (2010) and Farnbach (2017), I downloaded atmospheric models for brown dwarfs given in Saumon and Marley (2008) and Morley *et al.* (2012). Each brown dwarf model calculated the flux that a brown dwarf would produce at different wavelengths. The models were created based on four parameters: the temperature, surface gravity, cloud thickness, and rate of convection, which are referred to as T_{eff}, g, f_{sed}, and k_{zz}, respectively. Each of these parameters affects the shape of the model spectra and needed to be included. For each model, solar metallicity was assumed for the chemical composition. Metallicity impacts the observed spectrum but current models are unable to accurately model the effects of

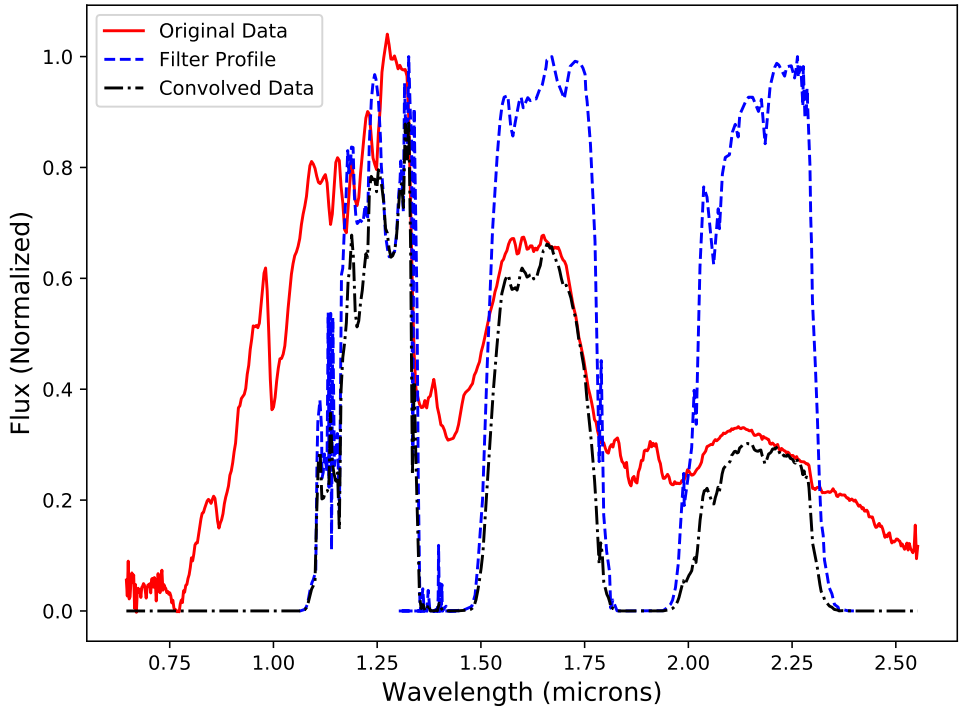

Figure 2.2 The convolution of spectral data and filter profiles for SDSS J1416+1348. The black line represents the convolution of the normalized data, shown in red, and the filter profiles, shown in blue. From left to right, the filter profiles correspond to the J, H, and K_s filters.

metallicity at this time.

Temperature directly affects the absorption features in the spectra, since certain molecules are more abundant in brown dwarfs of different temperatures. In the warmer L dwarfs, chemical reactions favor the production of CO over methane (CH_4) and we see strong absorption features from CO. But as the brown dwarf atmosphere cools, the production of CH_4 begins to dominate over CO and we see the CO absorption bands weaken as the CH_4 bands become more dominant. This difference occurs because in the hotter brown dwarfs, the thermal energy is high enough to break up the weak molecular bonds of methane. Similarly, other molecules, like ammonia (NH_3),

become more prevalent in cooler atmospheres and we see their spectral features become dominant below 800 K, as more nitrogen atoms are found in ammonia than in diatomic nitrogen. For this reason, temperature was key in determining the absorption features in brown dwarf spectra and was included as a factor to determine the shape of the model spectra. Temperature values that were used in the models were selected from a range from T_{eff} = 500 K to T_{eff} = 2400 K in increments of 100 K.

The surface gravity also affects the spectrum of the brown dwarf, as it determines the broadening of the absorption lines in the spectra. When the surface gravity, g, of an object is higher, larger pressure broadening occurs in the atmosphere and the spectral lines are broader. To account for the changes in the spectral shape due to surface gravity, the models also included g as a parameter. The models I used had a range of $\log(g)$ values from 3.75 to 5.5 in cgs units.

The density of clouds in the atmosphere and the rate of convection affect the spectra as well. Cloud density matters because thicker clouds can block light coming from the center of a brown dwarf. Convection is important because the intensities of the absorption lines change when clouds mix frequently and holes can develop, revealing deeper and hotter atmosphere layers. When mixing is common, certain molecules are pulled low into the atmosphere and since the regions closer to the center of the brown dwarf are warmer, the molecular bonds can be broken due to the higher thermal energy. For these reasons, the amount of cloud cover and the amount of mixing were also included in the models. The amount of cloud cover, f_{sed}, was defined as being an integer value between f_{sed} = 1 and f_{sed} = 5, where 1 corresponded to the highest density of clouds and 5 corresponded to the lowest density of clouds. There were also models which predicted the spectrum for brown dwarfs without clouds. The mixing constant, k_{zz}, was defined as an integer from k_{zz} = 0, to k_{zz} = 6, where 0 represented no mixing in the atmosphere and 6 represented the highest level of convection in the atmosphere.

Each model predicted the spectrum that would be given by a brown dwarf with a unique

combination of these properties. The title of each model included the values for T_{eff}, $\log(g)$, f_{sed}, and k_{zz}. When there were no clouds included in the model, the title of the model included the letters "nc" instead of an integer value for f_{sed}.

2.4 Adjusting the Atmospheric Models

Each model predicted the spectrum that would be given by a single brown dwarf, but I wanted to have models for binary brown dwarf systems as well. I used a code implemented by Farnbach (2017) to create binary models by combining all realistic combinations of the singular spectra. The fluxes for the singular models were added together to create these binary models. Since the brown dwarfs in a binary system would be at the same distance from Earth, the drop in flux from each brown dwarf to Earth would be the same, so the fluxes in the spectra could be simply added together without having to multiply by a constant. Therefore, in creating binary models, the fluxes at each wavelength of the two singular models were added together to create the binary model, as illustrated in Figure 2.3.

The models created by Saumon and Marley (2008) and Morley *et al.* (2012) were given with a very high resolution, and needed to be smoothed to match the spectral data collected. The models had data points every 0.01 nm while the spectra collected from IRSA, SPL, and the IRTF Spectral Library were of much lower resolution. Data from SPL and the IRTF Spectral Library had data points every 1-5 nm and IRSA data had data every 10-70 nm. The code created to fit the models would not function properly if the resolutions did not match. To resolve this, I used a code that read in the observed spectrum and the models and then smoothed the models to have the same resolution as the observed data.

The models were smoothed using a combination of two programs. The first program took every fortieth data point in the models and calculated the average of the 40 points to the right and the 40

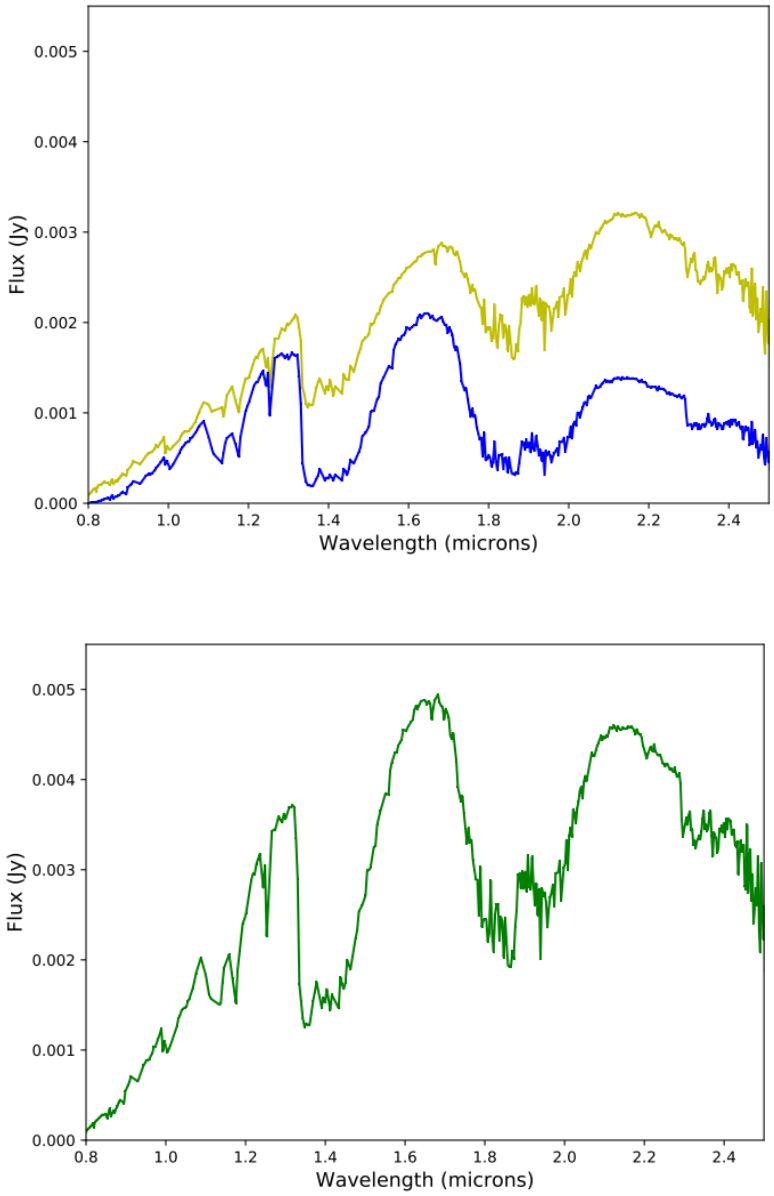

Figure 2.3 Two singular spectral models, shown in blue and yellow in the top graph, are added together to create a binary model, shown in green in the bottom graph.

points left of that point. The data point at that wavelength was then defined to the be the average value that was calculated, and a slightly lower resolution model was created. This was done to

decrease computation time for the second program, as there were hundreds of thousands of data points in each model. The lower resolution model was then read into another code that compared the lower resolution model against the spectral data and used spline interpolation between each point of the lower resolution model to determine where the model would have a data point at each of the wavelengths of the observed spectrum. These estimates were listed together to create the final model that had the exact same resolution as the observed spectrum. An example of a raw model compared to the final model created by the code is shown in Figure 2.4. Once the new models were created, they were collected into a separate folder, since each brown dwarf system required models with different resolutions.

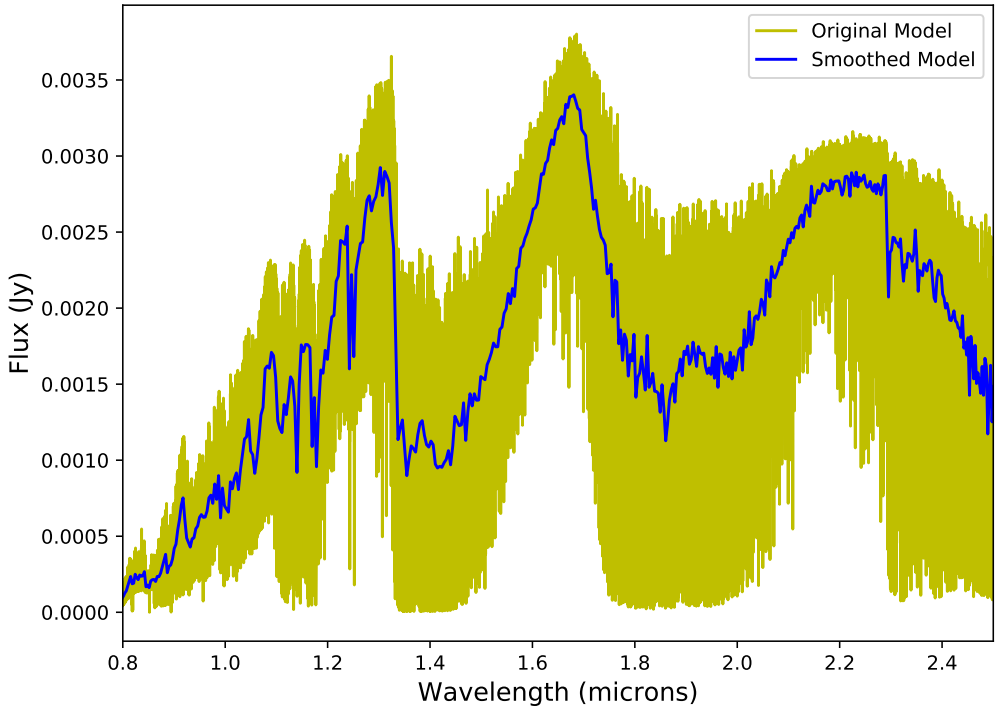

Figure 2.4 The smoothing of an atmospheric model to better fit the resolution of spectral data for the brown dwarf 2MASS 08053189+4812330 (2MASS 0805+4812). The original high-resolution is shown in yellow, and the model with the same resolution as the observed spectrum is shown in blue.

The observed data had a range of wavelengths where the data was not collected, since the data from SPL and the IRTF Spectral Library only included data up to 2.5 microns and data from IRSA started at 5 microns, as seen in Figure 2.5. When there were observational gaps in the data, the wavelengths of these gaps was given as an input to the fitting program, and the program ignored these wavelengths during the spectral fitting.

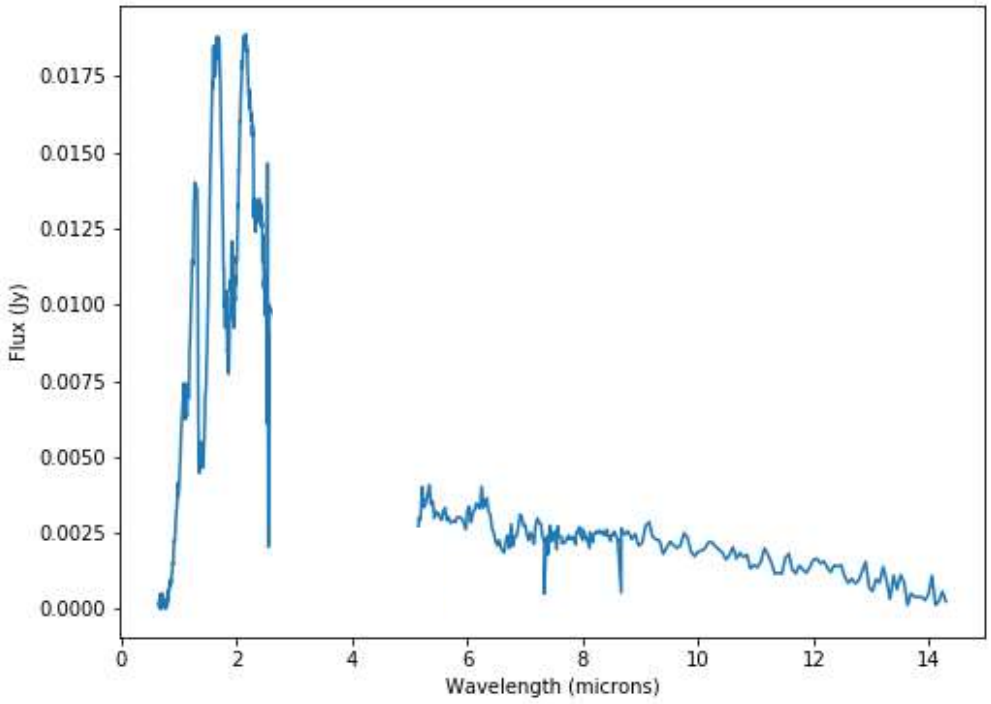

Figure 2.5 The spectrum of SDSSp J042348.57-041403.5 (SDSS 0423-0414). No spectral data between 2.5 and 5 microns was available, so this region of the spectrum needed to be ignored by the spectral fitting program.

2.5 Fitting Models to the Data

The singular and binary models were then fit to the spectral data, and a chi-squared analysis was performed. In a simple chi-squared analysis, models would be fit to the data and the differences between each of the data points and the points on the models would be squared and totaled together to determine the chi-squared value. For my analysis, a similar value was calculated, known as a G2 value. The G2 value was also a least-squared value, but it took into account the errors given in the data and the relative importance of each data point, multiplying each point by a normalized weight.

The formula for calculating the G2 value was the same used by Cushing *et al.* (2008) :

$$G2 = \sum_{\lambda} w(\lambda) \left[\frac{F(\lambda) - \alpha M(\lambda)}{\sigma(\lambda)} \right]^2 \quad (1)$$

In this equation, $F(\lambda)$ is the flux values of the observed spectra at each wavelength and $M(\lambda)$ is the predicted flux values given by the model at each wavelength. $\sigma(\lambda)$ is the error or amount of noise of each data point, and α is the constant to minimize the difference between the data and the model. The errors are included to account for the fact that the flux measured by each telescope at each wavelength has different observational errors. This minimizes the impact of data with lower signal-to-noise on the overall fit. The models predict the spectra at the surface of the brown dwarf. For a real brown dwarf, the luminosity at the surface drops off as a function of distance. To match theoretical models to real observed data, a constant offset (α) is applied to reduce the intensity of the model to match the flux we would observe for the object at Earth. This value is found during the fitting process and is a function of the true distance to the brown dwarf.

Due to the relative resolution between the short and the long wavelengths, weights for each wavelength were included, represented in the equation as $w(\lambda)$. The longer wavelength data collected from IRSA had less data points than the shorter wavelength data from SPL and the IRTF Spectral Library. If the data points from IRSA were not given a larger weight, they would have become insignificant to the fit. To make the longer wavelengths have an influence on the fit, the

weights were scaled according to the resolution of the data, so the longer wavelengths whose data points were more spaced apart were given a higher weight to increase their impact on the fit. The following equation implemented by Cushing *et al.* (2008) was used to determine the exact weight for each wavelength:

$$w = \frac{\Delta\lambda}{R} \tag{2}$$

In this equation, R is the total range of wavelengths compared, and $\Delta\lambda$ is the difference between the current wavelength and the wavelength before it. In this way, the weights were normalized so that $\sum w = 1$, as was established by Cushing *et al.* (2008) and Burgasser *et al.* (2010).

For each brown dwarf, the singular models were fit to the observed spectrum, and the G2 value for each singular model was calculated using a computer code. Once the G2 values were calculated, a list with each model's name and G2 value was created. The list was sorted, leaving the best fits with the smallest G2 values at the top of the list. The binary models were then fit to the spectral data using another code and the G2 values were calculated for each binary model. Since binary models were a combination of singular models, there were far more binary models than singular models. As such, only the models with the smallest G2 values were kept, to make the list easier to read. The G2 value for each model was calculated, and the 500 models with the lowest G2 values were listed and sorted according to their G2 values, again with the best fits at the top of the list.

After the binary models were fit to the spectral data, the results were compared to the fits of the singular models. I created a code to plot the models against the spectral data to see which models more closely matched the data. For each brown dwarf that I analyzed, I plotted the best singular model fit against the best binary model fit and the observed spectrum to visually discern the difference between the singular and binary models. Figure 2.6 shows a comparison between the best binary model fit, the best singular model fit, and the observed spectrum for the brown dwarf 2MASS 14313097+1436539 (2MASS 1431+1436). Figure 2.7 shows the best binary model fit, the best singular model fit, and the spectral data for the brown dwarf 2MASS 05591914-1404488

(2MASS 0559-1404), with both the 0.6-2.5 micron and 5-14.5 micron ranges included. For these brown dwarfs, the binary models fit the data better than the singular models. Though the differences between the models appeared minuscule in the graphs, the small disparities could add up to make a significant difference in the overall fit. Since human perception was not accurate in determining the goodness of fits for these graphs, I used statistics to determine the confidence level at which a binary fit was better than a singular fit for each brown dwarf.

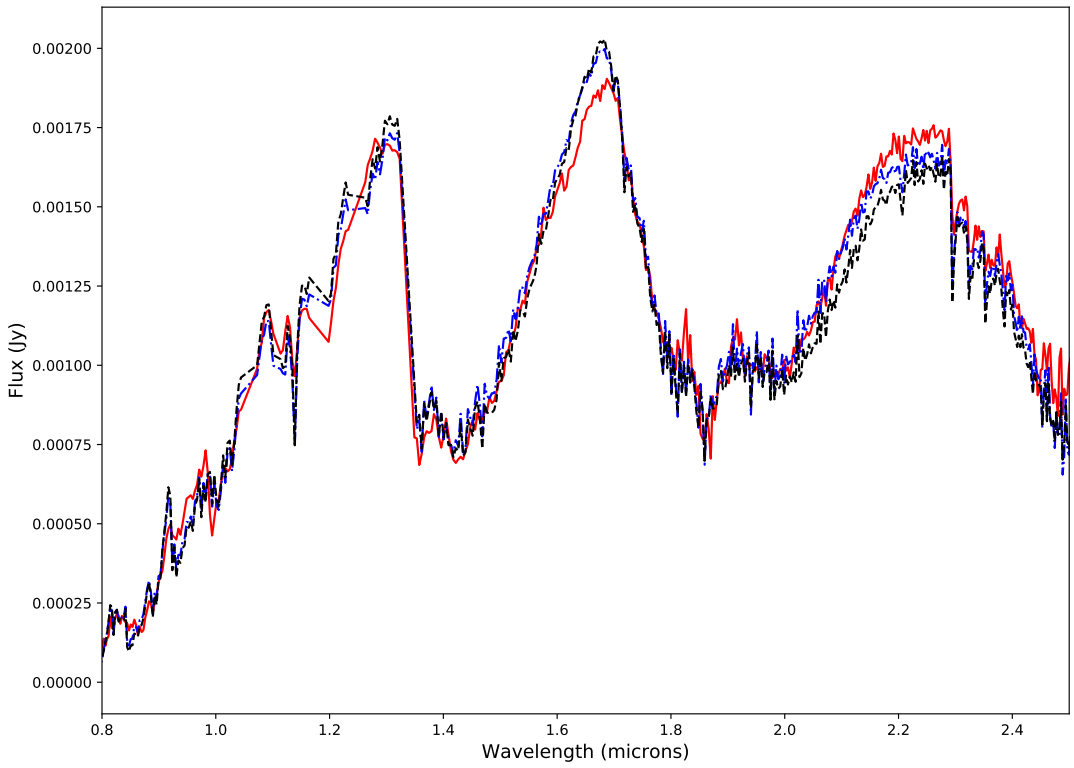

Figure 2.6 The best fits for singular and binary spectral models compared to the observed spectrum for 2MASS 1431+1436. The observed spectrum is shown in red, the singular model in black, and the binary model in blue. A distinction between the singular and binary models is best seen at the wavelength of 2.2 microns, where the binary model is closer to the observed spectrum that the singular model.

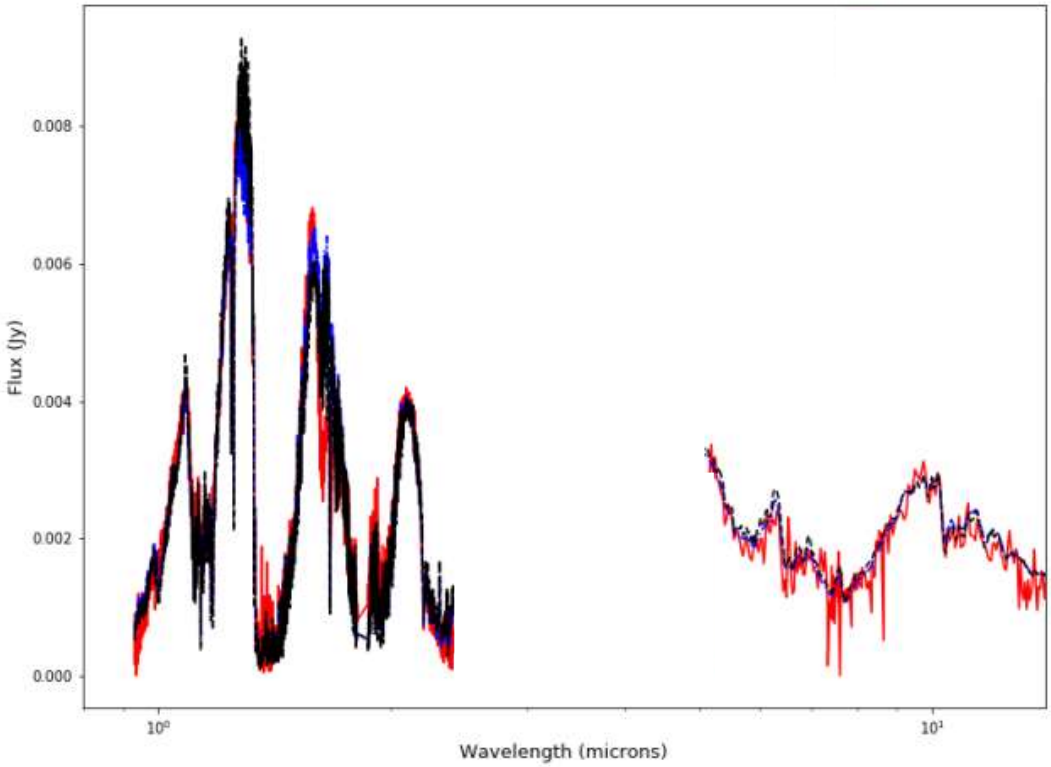

Figure 2.7 The best fits for singular and binary spectral models compared to the observed spectrum for 2MASS 0559-1404. The observed spectrum is shown in red, the singular model in black, and the binary model in blue. A full range of wavelengths is shown here and includes data over the range of 0.6-2.5 microns and 5-14.5 microns. A logrithmic scale is used to see the spectrum at the shorter wavelengths better.

2.6 Statistical Analysis

A one-sided F-test was performed to determine the validity of the claim that a system was binary.

As was done by Burgasser *et al.* (2010), I used the distribution statistic

$$\eta_{\rm sb} = \frac{\min(G2_{\rm sing})/\nu_{\rm sing}}{\min(G2_{\rm bin})/\nu_{\rm bin}} \tag{3}$$

Here, ν is the number of degrees of freedom, G2 is the value calculated in equation (1) and the subscripts sing and bin refer to singular and binary models, respectively. For unweighted data, the number of degrees of freedom could be calculated as $\nu = N - 1$ where N would be the number of data points. However, due to the weights I used, each point contributed a different amount to the G2 value. Knowing this, I calculated the degrees of freedom using the equation

$$\nu = \left[\frac{1}{\max(w(\lambda))} \sum_{\lambda} w(\lambda) \right] - 1 \tag{4}$$

as established by Burgasser *et al.* (2010). In the equation, $w(\lambda)$ is the weight for each wavelength, given by equation (2). Since both models had the same resolution and therefore the same weights, $\nu_{\rm sing} = \nu_{\rm bin}$ and the ratio for $\eta_{\rm sb}$ became

$$\eta_{\rm sb} = \frac{\min(G2_{\rm sing})}{\min(G2_{\rm bin})} \tag{5}$$

For each of the brown dwarfs studied, the ratio between the best singular and binary fits was calculated to determine $\eta_{\rm sb}$. Then, using the degrees of freedom calculated, the F-distribution probability distribution function for each system was established, using a code I created. I then found the level of confidence at which the value of $\eta_{\rm sb}$ predicted the brown dwarf system to be binary. An example of a probability distribution function for the brown dwarf SDSSp J042348.57-041403.5 (SDSS J0423-0414) is shown in Figure 2.8. The values of $\eta_{\rm sb}$ at which the system could be determined to be binary at the 90%, 95%, and 99% confidence levels are also shown. When I studied the $\eta_{\rm sb}$ values for the brown dwarf systems, I noted the systems with $\eta_{\rm sb}$ values above the 90% level as targets of interest, and ruled out the null hypothesis that the system was singular when $\eta_{\rm sb}$ exceeded the 99% confidence level.

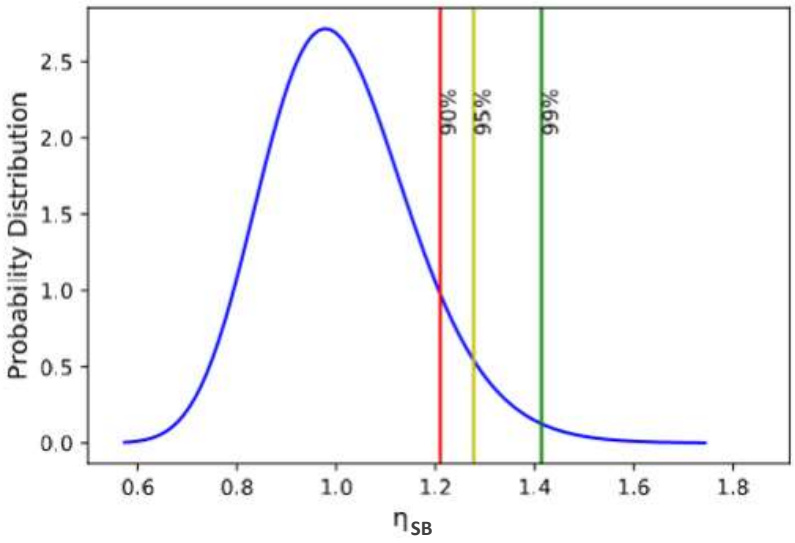

Figure 2.8 The probability distribution for the F-statistic $\eta_{\rm sb}$ for SDSS J0423-0414. The vertical lines show the values that $\eta_{\rm sb}$ must pass to surpass the different levels of confidence, with a value surpassing 99% being the point at which the null hypothesis of a system being a single brown dwarf is rejected. The distribution changes based on the number of degrees of freedom in the models.

Chapter 3

Results and Future Work

3.1 Identified Binary Systems

By identifying overluminous systems, a list of 117 brown dwarf candidates was created. Of these 117 systems, 26 had spectra available on the public spectral archives. There were 19 systems that had data in only the 0.8-2.5 micron range, while the other seven systems had data in both the 0.8-2.5 micron and 5-14.5 micron range. I ran the spectral fitting and statistical analysis codes on these 26 systems and seven were found to be binary at the 99% confidence level. Three systems were found to be binary above the 95% confidence level and two above the 90% confidence level. All these candidates were noted as targets of interest, while the systems that did not pass the 90% confidence were disregarded. A summary of the binary systems discovered and the level of confidence at which they were identified is shown in Table 3.1.

The fitting of models to the spectral data not only helped determine whether a system was binary, but it also provided insight into the physical parameters of each component of the binary system. A list of the brown dwarf systems that were found to be binary above a 99% level are listed in Table 3.2. The table also includes the combination of models that created the best binary fit, listing

the model with the larger flux as the primary model and the model with the smaller flux as the secondary model. The models are listed as a combination of the properties that made them: T_{eff}, $\log(g)$, f_{sed}, and k_{zz}. The units and description of these properties are given in Chapter 2.

From Table 3.2, similarities between the binary systems can be identified. Three of the systems have brown dwarfs that have similar temperatures. Each of the other four systems each has a combination of an L and a T dwarf. The surface gravities for all of the brown dwarfs are high. Further research could show if these properties are always prevalent in binary systems.

The singular model fits for these systems are also listed, in Table 3.3. Overall, the temperatures for the singular model fits were close to the temperatures of the binary model fits. For binary fits where the temperatures of the two brown dwarfs were close or identical, the singular fits gave temperatures that were equal to or only 100 K off from the two brown dwarfs in the binary models. For systems that had binary fits of brown dwarfs with largely different temperatures, the singular fits gave temperatures that were equal to or only 100 K different from the temperature of the primary models of the binary fits. The comparison between binary and singular models shows that both are good predictors of the temperature of brown dwarf systems, but that singular models favor the primary brown dwarf in binary systems. From analyzing the binary fits, I deduced that many binary systems could be hard to detect for two reasons: either they have two brown dwarfs that are similar in temperature, making it difficult to discern the difference between the brown dwarfs, or they have one brighter brown dwarf that makes it hard to see its dimmer companion.

The optical spectral types for the binary systems discovered are also included for comparison in Table 3.3. The spectral types can be compared to the temperatures of the fits to see if the fits are accurate, meaning that the temperatures of the models correspond to the correct spectral type.

As more brown dwarf binary systems are found and studied, we can continue to to look for correlations between the physical parameters of the primary and secondary objects, their relative separation, cloud properties, etc. To discover such correlations would require far more data than I

have been able to study, but using the methods I have outlined, such research could be done.

3.2 Comparison to Previous Results

To test the accuracy of the discovery process and the computer code, I tested systems identified as being binary by other researchers. Burgasser *et al.* (2010) studied systems using a method similar to the one outlined in this thesis and also identified the level of confidence at which these systems were identified as binary. However, instead of comparing observed spectra to models, he compared them to real data. This approach, while presumably more accurate, is more difficult than mine, because there are a limited number of brown dwarf spectra that could be used for comparison. I wanted to see if my method of using models instead of real data would be just as accurate and identify the same systems as binary, as this would verify my work. Burgasser identified 17 systems being as being binary at the 99% confidence level, and of these 17, I found 15 to be binary at the same level of confidence and one to be binary at a 95% confidence level. My results differed significantly from Burgasser's for the systems SDSS J075840.33+324723.4 (SDSS J0758+3247) and SDSS J120747.17+024424.8 (SDSS 1207+0244), however. I found SDSS J0758+3247 to be binary at the 99% confidence level but Burgasser did not find it be binary, even at the 90% confidence level. Conversely, I did not find SDSS 1207+0244 to be binary, even at the 90% confidence level, while Burgasser found it to be binary at the 99% confidence level. While not a perfect match, my results mostly agreed with those given by Burgasser. This is a confirmation that models, for the most part, can be as good at finding binaries as actual data. A comparison of Burgasser's results and my results for several brown dwarf systems is shown in Table 3.4.

The system 2MASS 0559-1404 is another target of interest that has been identified as being a possible binary system. Research done by Esplin (2010) with spectroscopy and current research by Denise Stephens' research group with photometric analysis indicate that the system is binary. My

results agreed with theirs, as I identified the system as being binary above a 99% confidence level.

The code I used proved to be fallible with my study of the Kelu-1 system. The Kelu-1 system has been previously identified as a binary system using photometry. However, by using spectral analysis, I did not find it to be binary, even at the 90% confidence level. A possible reason for this discrepancy is that the two brown dwarfs in the Kelu-1 system have similar temperatures. The best binary fit was found to be from a model combining two spectra with temperatures that were both 1800 K. Since temperature causes the main difference between models, the two models used in the binary model appeared similar to the singular model and made it difficult to discern a difference between the binary and singular models. Yet, as can be seen in Table 3.2, other systems that had dwarfs with similar temperatures were found, so this may not be the only reason that the code failed to find Kelu-1 to be binary. Another possible reason is that Kelu-1 is a system with a hot L dwarf. The models I used only went up to temperatures of 2400 K. If the temperature of the system exceeded this temperature, the models would not have accurately modeled the spectrum. Thus, the fitting code is not conclusive, since a system could be binary even if the code does not find it to be.

3.3 Future Work

Though effective, the code I used could still be improved. Three different parts of the code had been written in different coding languages and needed to be run separately in order to function properly. To make the process quicker, the code could be rewritten to be all in one language. The different stages of smoothing the models, fitting the models, and performing the statistical analysis could be automated in a pipeline to make them all run with a single line of code in a Linux terminal. By creating this pipeline, the time it would take to identify binary systems could be significantly reduced.

Such a reduction in time spent in running the code would be helpful to achieve the greater

Table 3.1 Confidence Levels for Discovered Binary Systems

Name	η_{sb}	Confidence Level
2MASS 05591914-1404488	1.554	99%
SDSS J042348.57-041403.5	1.549	99%
2MASSW J0320284-044636	1.520	99%
2MASS 14313097+1436539	1.449	99%
DENIS-P J225210.73-173013.4	1.355	99%
2MASS 20282035+0052265	1.287	99%
SDSS J141624.08+134826.7	1.257	99%
SDSSp J125453.90-012247.4	1.323	95%
Gl 417 BC	1.244	95%
2MASS 09153413+0422045	1.181	95%
2MASS 20360316+1051295	1.161	95%
WDS J15200-4423A	1.146	90%

purpose of this research, which is to develop a better evolutionary model for brown dwarfs. The methods I used can be followed to discover more binary systems efficiently. By discovering more binary systems and identifying their proprieties, correlations between their properties can be created. When enough systems are studied, a more accurate model for the formation and evolution of brown dwarfs can be created and can help astronomers to better understand the nature of these celestial bodies.

Table 3.2 Best Fit Binary Models for Discovered Binary Systems

Name	Primary T_{eff} / $\log(g)$ / f_{sed} / k_{zz}	Secondary T_{eff} / $\log(g)$ / f_{sed} / k_{zz}
2MASS 05591914-1404488	1200 / 5.5 / 4 / 0	1200 / 5 / nc / 0
SDSS J042348.57-041403.5	1500 / 5.5 / 2 / 0	1500 / 5.5 / 4 / 6
2MASSW J0320284-044636	2400 / 4.5 / 1 / 2	1600 / 5.5 / 1 / 0
2MASS 14313097+1436539	2300 / 4.5 / nc / 0	1400 / 5.5 / 3 / 4
DENIS-P J225210.73-173013.4	1700 / 5 / 1 / 2	1200 / 5.5 / 4 / 2
2MASS 20282035+0052265	1600 / 5.5 / 3 / 4	1500 / 4.5 / 1 / 0
SDSS J141624.08+134826.7	1900 / 5.5 / 4 / 0	1200 / 5.5 / 4 / 6

Table 3.3 Best Fit Singular Models and Optical Spectral Types for Discovered Binary Systems

Name	Single T_{eff} / $\log(g)$ / f_{sed} / k_{zz}	Optical Spectral Type
2MASS 05591914-1404488	1200 / 5.5 / 5 / 0	T5
SDSS J042348.57-041403.5	1400 / 5.5 / 3 / 6	L7.5
2MASSW J0320284-044636	2400 / 3.5 / 1 / 0	M8
2MASS 14313097+1436539	2200 / 3.5 / 2 / 0	L2
DENIS-P J225210.73-173013.4	1600 / 5.5 / 3 / 0	Unknown
2MASS 20282035+0052265	1600 / 5.5 / 2 / 4	L3
SDSS J141624.08+134826.7	1800 / 5.5 / 4 / 0	L6

Table 3.4 Comparison of Confidence Levels for Binary Systems

Name	My η_{sb}	My Confidence Level	Burgasser's Confidence Level
SDSS J011912.22+240331.6	1.430	99%	99%
SDSS J024749.90-163112.6	2.433	99%	99%
SDSS J035104.37+481046.8	1.558	99%	99%
SDSS J090900.73+652527.26	1.302	99%	99%
2MASS J09490860-1545485	1.231	95%	99%
SDSS J103931.35+325625.5	1.596	99%	99%
2MASS J11061197+2754225	1.881	99%	99%
SDSS J120747.17+024424.8	1.051	<90%	99%
2MASS J13243559+6358284	1.918	99%	99%
SDSS J141530.05+572428.7	2.483	99%	99%
SDSS J143553.25+112948.6	3.122	99%	99%
SDSS J143945.86+304220.6	1.783	99%	99%
SDSS J151114.66+060742.9	1.533	99%	99%
SDSS J151603.03+025928.9	1.328	99%	99%
2MASSI J1711457+223204	1.320	99%	99%
SDSS J205235.31-160929.8	1.420	99%	99%
2MASS J21392676+0220226	1.734	99%	99%
SDSS J120602.51+281328.7	1.343	99%	90%
SDSS J151643.01+305344.4	1.088	<90%	<90%
SDSS J075840.33+324723.4	2.020	99%	<90%

Bibliography

Burgasser, A. J., Cruz, K. L., Cushing, M., Gelino, C. R., Looper, D. L., Faherty, J. K., Kirkpatrick, J. D., & Reid, I. N. 2010, The Astrophysical Journal, 710, 1142

Cushing, M. C., et al. 2008, The Astrophysical Journal, 678, 1372

Esplin, T. L. 2010, Statistical Spectral Fitting of the Brown Dwarf Binary System 2M0559, Brigham Young University, [Bachelor's Thesis]

Farnbach, L. T. 2017, Statistical Spectral Fitting of Potential Brown Dwarf Binary System, Brigham Young University, [Bachelor's Thesis]

Gagliuffi, D. C. B., & Burgasser, A. J. 2014, The Astrophysical Journal, 794, 143

Morley, C., Fortney, J. J., Marley, M. S., Visscher, C., Saumon, D., & Leggett, S. K. 2012, The Astrophysical Journal, 756, 172

Phillps, M., et al. 2020, arXiv e-prints, arXiv:2003:13717

Rebolo, R., Osorio, M. Z., & Martin, E. 1995, Nature, 377, 129

Saumon, D., Marley, M., Lodders, K., & Freedman, R. 2003, The Astrophysical Journal, 211, 345

Saumon, D., & Marley, M. S. 2008, The Astrophysical Journal, 689, 1327

Stephens, D., et al. 2009, The Astrophysical Journal, 702, 154

Thies, I., Pflamm-Altenburg, J., Kroupa, P., , & Marks, M. 2015, The Astrophysical Journal, 800, 72

Index

atmospheric models, 11

binary models, 14
brown dwarf desert, 3
brown dwarf formation, 1

Combined Atlas of Sources with Spitzer IRS Spectra, 9

degrees of freedom, 22

effective temperature, 2

F-test, 21
filter profile, 10

G2 value, 18
Gaia, 4

InfraRed Science Archive, 9
InfraRed Spectrograph, 9
InfraRed Telescope Facility, 9
Initial Mass Function, 3

Jansky, 10

Keck Observatory Archive, 9

normalized spectra, 10

overluminous, 4

probability distribution function, 22

spectral types, 2
spectrograph, 7
Spitzer Space Telescope, 5, 9

Wein's law, 8